JSHC
Japan Society of
Histochemistry and Cytochemistry
Established 1959

Acta Histochem. Cytochem. 50 (1): 29–37, 2017
doi: 10.1267/ahc.16024

Expression of Nicotinic Acetylcholine Receptor α4 and β2 Subunits on Direction-Selective Retinal Ganglion Cells in the Rabbit

Jun-Seok Lee[1,*], Hyun-Jin Kim[2,*], Chang-Hyun Ahn[1,*] and Chang-Jin Jeon[1]

[1]Department of Biology, School of Life Sciences, BK21 Plus KNU Creative BioResearch Group, College of Natural Sciences, and Brain Science and Engineering Institute, Kyungpook National University, Daegu 41566, South Korea and [2]Department of Life Sciences, Pohang University of Science and Technology, Pohang 37673, Kyungpook, South Korea

Received July 27, 2016; accepted December 26, 2016; published online February 22, 2017

The direction selectivity of the retina is a distinct mechanism that is critical function of eyes for survival. The direction-selective retinal ganglion cells (DS RGCs) strongly respond to a preferred direction, but rarely respond to opposite direction or null directional visual stimuli. The DS RGCs are sensitive to acetylcholine, which is secreted from starburst amacrine cells (SACs) to the DS RGCs. Here, we investigated the existence and distribution of the nicotinic acetylcholine receptor (nAChR) α4 and β2 subunits on the dendritic arbors of the DS RGCs in adult rabbit retina using immunocytochemistry. The DS RGCs were injected with Lucifer yellow to identify their dendritic morphology. The double-labeled images of dendrites and nAChR subunits were visualized for reconstruction using high-resolution confocal microscopy. Although our results revealed that the distributional pattern of the nAChR subunits on the dendritic arbors of the DS RGCs was not asymmetric in the adult rabbit retina, the distribution of nAChR α4 and β2 subunits and molecular profiles of cholinergic inputs to DS RGCs in adult rabbit retina provide anatomical evidence for direction selectivity.

Key words: direction selectivity, nicotinic acetylcholine receptor, retinal ganglion cell, cell injection, immunocytochemistry

I. Introduction

Motion detection is essential for animal survival. For this purpose, mammalian eyes have a special functional response to selective direction of movement from a subset of retinal ganglion cells called the direction-selective retinal ganglion cells (DS RGCs). The DS RGCs respond strongly to an object that moves in a preferred direction, but respond weakly or not at all to stimuli moving in an opposite (null) direction [3, 8, 10, 13, 15, 22, 33, 52, 53]. Since the discovery of direction selectivity in the retina by Barlow and Hill in 1963, its underlying mechanisms have been intensively studied for last five decades how direction selectivity is implemented [9, 10, 13, 15, 34, 42, 55]. The DS RGCs have been especially well studied in rabbit retina, with a focus on the ON-OFF DS RGCs. These cells have bistratified dendrites at a depth of 20% and 70% of the inner plexiform layer (IPL) of the retina in sublamina a (OFF) and sublamina b (ON), respectively [7, 11, 13, 29, 49, 50, 57]. With their distinctive anatomical structures, various receptors are expressed in the ON-OFF DS RGCs [26, 28, 30, 31, 44], but the molecular profiles of the ON-OFF DS RGCs are not fully understood.

The major mechanism of direction selectivity is known to mediate strongly with starburst amacrine cells (SACs), which are functionally hard-wired to the DS RGCs through both cholinergic and GABAergic synapses to allow for asymmetrical directional selectivity [5, 10, 15, 18, 34, 56]. The SACs are a cholinergic interneuron that co-release acetylcholine (ACh) and γ-aminobutyric acid (GABA) to

* These authors contributed equally to this work.

Correspondence to: Prof. Chang-Jin Jeon, Ph.D., Neuroscience Laboratory, Department of Biology, College of Natural Sciences, Kyungpook National University, 80 Daehak-ro, Buk-gu, Daegu 41566, South Korea.
E-mail: cjjeon@knu.ac.kr

the dendrites of the ON-OFF DS RGCs [16, 39]. Recent studies reported that asymmetric synaptic contact between SACs and DS RGCs highly correlates with a null direction, which provides direction selectivity to the DS RGCs [10, 49, 55]. In addition to studies demonstrating the GABAergic inhibition from the SACs to the ON-OFF DS RGCs, other studies propose that ACh has a major role in the functional computation of the microcircuit for the directional information [19]. Moreover, another study revealed that ACh and specific ACh receptor subunits are critical for induction of direction selectivity in the retina [45]. However, it is unknown which ACh receptor subunits are expressed upon the dendrites of the ON-OFF DS RGCs.

Nicotinic acetylcholine receptors (nAChRs) are ligand-gated ionotropic receptors. They are comprised of a pentamer with combinations of nine α subunits (α2–α10) and three β subunits (β2–β4). The nAChRs are usually assembled $(\alpha7)_5$ only in a homomeric or binary complex, while $(\alpha3)_2(\beta4)_3$ and $(\alpha4)_2(\beta2)_3$ nAChRs are assembled as heteromeric receptors in the central nervous system [1, 35, 48]. These nAChRs, which contribute to the preferred direction excitation of the ON-OFF DS RGCs, are reduced their preferred responses by employing the nicotinic antagonist curare [19]. Consistent with this influence of the nAChRs on the ON-OFF DS RGCs, pharmacological and physiological investigations show that some subunits of the nAChR, specifically the nAChR α7 and β2 subunits, contribute significantly to direction selectivity through expression on dendrites of the ON-OFF DS RGCs [45]. However, the distributional pattern for direction selectivity according to the expression of nAChR subunits on dendrites of the ON-OFF DS RGCs is unknown; thus, further study is necessary to identify the presence of additional nAChR subunits. Investigation of the nAChR α4 and β2 subunits, which canonical co-expressed subunits in the mammalian central nervous system, may provide clues for understanding the mechanism of the direction selectivity because it is one of the earliest expressed nAChR subunits, which is increased expression during developmental stages in the retina [38].

The purpose of the present study was to investigate the distributional pattern of the nAChR α4 and β2 subunits in the adult rabbit retina. To achieve our goal, we injected to DS RGCs with Lucifer yellow and performed immunocytochemistry on vibratome sections and whole mounts of rabbit retina. The double-labeled images of dendrites and nAChR subunits were visualized using confocal microscopy. We revealed the expression of the nAChR α4 and β2 subunits upon the dendritic arbors of DS RGC; however, the distributional patterns of these subunits upon dendrites of both the ON and OFF layers of the DS RGCs in the adult rabbit retina were not asymmetric.

II. Materials and Methods

Experimental preparations and retinal isolation

Approximately 24 hr before the experiment, an adult New Zealand white rabbit ($N = 1$ animal) was anesthetized using a mixture of xylazine (15 mg/kg) and ketamine (75 mg/kg). To select the DS RGCs, both eyes of the rabbit were injected with 10 μg of the fluorescent marker 4',6-diamidino-2-phenylindole (DAPI) and were acclimatized to darkness. This procedure helps discriminate the SACs from the ganglion cells using strong DAPI signal. One day later, the dark-adapted rabbits were re-anesthetized with the same mixture of ketamine and xylazine. The eyes were immediately enucleated and hemisected at the equator, and the retinas were isolated attentively from the pigmented epithelium. These experimental procedures were carried out in Ames' medium (Sigma-Aldrich Co., St. Louis, MO, USA) that had been equilibrated with 95% O_2 and 5% CO_2 [2, 53] for maintaining live rabbit retina cells *in vitro*. This technique was developed and described in detail by Masland and Ames [36], and Ames and Nesbett [2]. All investigations involving animals were performed in accordance with the guidelines of the Association for Research in Vision and Ophthalmology (ARVO) statement for the Use of Animals in Ophthalmic and Vision Research.

Living cell injection using Lucifer yellow

To wash residues of unbound DAPI from the retina, the isolated retina was rinsed with Ames' medium for 10 min. After this procedure, the retina was placed on a piece of the non-fluorescent filter membrane (0.45 μm, Black, HABP 47 mm; Millipore, Billerica, MA, USA) with the ganglion cell layer (GCL) on the upper side. The mounted retina was immersed in a superfusion chamber that kept the fresh Ames' medium flowing for maintaining the living cells of the retina, and a platinum ring was placed on the membrane to prevent movement. The chamber was positioned on the stage of a Zeiss fixed-stage fluorescence microscope. Under fluorescent illumination, we injected 5% Lucifer yellow into the candidate cells, which had a large somata and a kidney-shaped nucleus. These distinctive cells are highly likely to be the ON-OFF DS RGCs [53]. Additionally, the mid-peripheral region of the retina was targeted for injection to avoid a high density of blood vessels. Targeted cells were injected with 5% Lucifer yellow using conventional techniques [21, 26, 53]. Lucifer yellow was injected into the cells via iontophoresis, and then we selected the cells with a distinctive morphology of their dendritic arbors, which is the characteristic honeycomb of the ON-OFF DS RGCs and the bistratified appearance. As no other neuron with these characteristics has been reported in the rabbit retina, these features unambiguously differentiate the ON-OFF DS RGCs from all other known types of RGCs in rabbits.

Fluorescence immunocytochemistry

After the intracellular injection, the retinal tissue was fixed with 4% paraformaldehyde in 0.1 M phosphate buffer (pH 7.4) for 2 hr. We conducted conventional immunocytochemical techniques that we have previously described in detail [24]. Through this method, we identified the distributions and localization of retinal ganglion cells in mouse and rabbit [32, 54]. Briefly, the fixed retinal tissues were rinsed three times with 0.1 M phosphate buffer, and were incubated with a blocking solution (4% normal serum of the secondary antibody host, 0.4% Triton X-100 added in 0.1 M phosphate buffer) for 1 day. The treated rabbit retinal tissues were then labeled with the primary antibodies against the nAChR α4 subunits (SC-1772; 1:100; Santa Cruz Biotechnology, Inc., Santa Cruz, CA, USA) or β2 subunits (SC-11372; 1:100; Santa Cruz Biotechnology, Inc.) for 3 days. Subsequent to washing three times again with 0.1 M phosphate buffer, the tissues were incubated for 1 day with secondary antibodies, including Cy5-conjugated rabbit anti-goat IgG (1:50; Jackson ImmunoResearch Laboratories, Inc., West Grove, PA, USA) for the α4 subunits and Cy5-conjugated goat anti-rabbit IgG (1:50; Jackson ImmunoResearch Laboratories, Inc.) for the β2 subunits. Some vertical sections were incubated in the same solution without the primary antibodies. After immunocytochemistry, the tissues were washed three times in 0.1 M phosphate buffer, and were coverslipped with Vectashield mounting media (Vector Laboratories, Inc., Burlingame, CA, USA). Vertical tissue sections were prepared by Vibratome sectioning (Vibratome 3000 Plus, Vibratome, St Louis, MO, USA). The whole retina was embedded in 4% agarose gel and sliced at a thickness of 40–50 μm.

Data analysis

The Lucifer yellow-filled DS RGCs were imaged using a laser-scanning confocal microscope (MRC 1024; Bio-Rad Laboratories, Inc., Hercules, CA, USA) that was equipped with either a 40× objective (NA 0.75; Plan Fluor; Nikon, Tokyo, Japan) or 20× objective (NA 0.50; Plan Fluor; Nikon). We used Z-axis serial imaging to discriminate the puncta and the ON and OFF layer of each DS RGC. For the average density of immunoreactive puncta at the ON and OFF layer, we used a threshold image analysis with the Image-J program, version 1.48 (Wayne Rasband, National Institutes of Health, Bethesda, MD, USA). The immunopuncta images from the ON and OFF layers of the DS RGCs were imported into Image-J, then we applied a threshold color function (Threshold color: Red; Color space: HSB; Hue: 0–255, Saturation: 0–255; Brightness: 165–225; Size [pixel]^2: 20-infinity), and counted the puncta that passed the criteria. For reconstruction of the entire shape of the DS RGCs, a series of high-resolution confocal images in the plane of each cell's ON and OFF dendritic layer was acquired through a Nikon Plan Fluor 100× objective (NA 1.30 oil; Plan Fluor; Nikon). To avoid crosstalk, we used an emission filters 515DF30 (Lucifer yellow: dendrites) and 680DF32 (Cy5: nAChR α4 and β2 subunits).

We obtained approximately 150–200 fields of confocal images for each ON and OFF dendritic layer in each cell and tiled these images to complete a 512 × 512 montage image. These images were tiled, and immunopuncta and dendrites were mapped onto transparent film to reconstruct the DS RGC images (Fig. 5). We identified the nAChR immunoreactive puncta, which were located upon the dendrites of the DS RGCs. The final images of the nAChR α4 and β2 subunits puncta were analyzed using Adobe Illustrator 10 (Adobe Systems, Mountain View, CA, USA). The details of this analysis procedure and our criterion for counting the immunoreactive puncta have been described in our previous reports [25, 26, 30, 32]. To briefly describe the puncta analysis, we calculated the nAChR subunits immunopuncta on the dendrites for each of the eight cardinal directions, and immunopuncta within 45° of a given cardinal direction were included in the histogram (Fig. 6). First, the densities of the nAChR α4 and β2 immunopuncta were presented in terms of the length of the dendrite (number of puncta/μm of a dendrite). For the histogram presentation, we calculated the puncta densities at 10 μm intervals from the center of the soma to the outer dendrites for each cardinal direction. Second, the average density of the nAChR subunits immunopuncta was expressed in terms of the number of immunoreactive puncta per total μm length of the dendrites within each cardinal direction. To estimate the precise spatial symmetry of the nAChR subunits immunoreactive puncta upon the DS RGCs, we calculated a symmetry index (SI) as described in previous studies [28, 30]. The SI was calculated for each cell using the formula SI = 10(B/A) for (B < A), where 'A' represents the average spatial density of the nAChR subunits immunopuncta in one of the eight cardinal directions of the DS RGCs, and 'B' represents the spatial density of the nAChR subunits immunopuncta on the dendritic arbor of the symmetrically opposite direction. We analyzed the SI value of the dendrites for all eight directions. The SI value of 10 would indicate complete symmetry, while the SI value of 0 would indicate a total asymmetry. We calculated the average SI of each DS RGC from the eight SI values, and quantified the results of two injected cells from one animal (Fig. 7).

The number of immunopuncta per unit distance was calculated using a simple method in which the total number of puncta was divided by the whole length of the dendritic plexus in each single cell (i.e., whole number of puncta on the DS RGC dendrites/whole length of dendrites in a single DS RGC). The whole length of dendrites was measured using the 'Analyze-Measure' function tool in the Image-J program, version 1.48 after setting the scale with a scale bar.

III. Results

To identify the DS RGCs, we applied the living cell

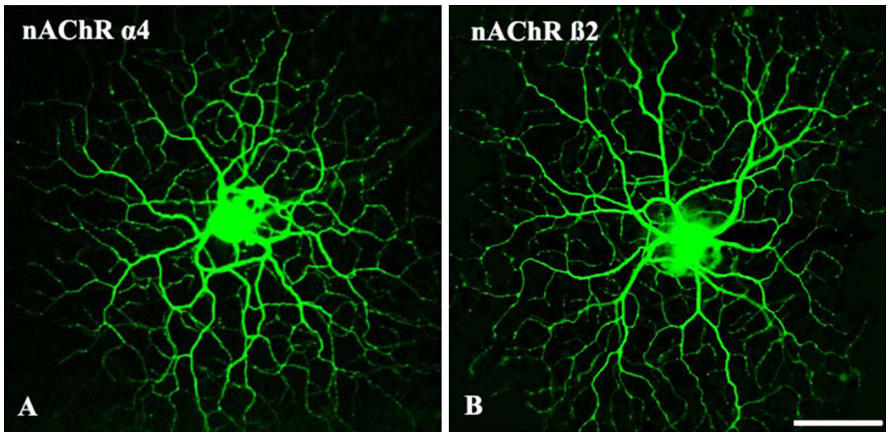

Fig. 1. The representative shape of the DS RGCs injected with 5% Lucifer yellow. In these photomicrographs, which were taken at a low magnification, both the ON and OFF dendritic arbors are visible. The two dendritic arbors in panels (**A**) and (**B**) were used to analyze the distributions of immunoreactivity for the nAChR α4 and β2 subunits, respectively. Bar = 100 μm.

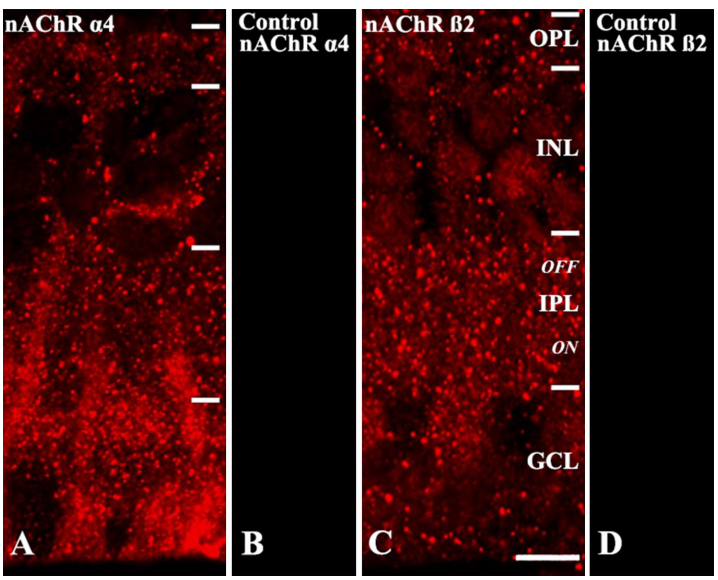

Fig. 2. Immunoreactivity of the nAChR α4 and β2 subunits in vertical vibratome sections of the mid-peripheral rabbit retinas. Fluorescence confocal micrographs show the immunopuncta labeled with antibodies against nAChR α4 (**A**) and nAChR β2 (**C**) subunits. Strong densities of immunoreactivity for nAChR α4 subunits were observed in the inner plexiform layer (IPL) and ganglion cell layer (GCL) (**A**). Strong immunoreactivity of the puntate for nAChR β2 subunits is also present in IPL (**C**). Some immunoreactive punctate for the nAChR α4 and nAChR β2 are observed in the outer plexiform layer (OPL), inner nuclear layer (INL), respectively. Incubated vertical sections without the primary antibodies showed no specific immunoreactivity (**B, D**). Bar = 10 μm.

injection technique, as shown in Figure 1. The cells in panels A and B were used to analyze the distribution of the nAChR α4 and β2 subunits in the adult rabbit retinas, respectively. Many types of ganglion cells in the mammalian retina have been studied [3, 46], and the DS RGCs of the mammalian retina have characteristic morphological properties. The overall dendritic arbors of the DS RGCs have a unique honeycomb appearance. Moreover, the DS RGCs are bistratified with an ON and OFF layer; one portion narrowly stratifies within sublamina a of the IPL, whereas the other ramifies narrowly within sublamina b [3, 4, 53]. In addition, the emerged terminal branches of the DS RGCs often curve back to point toward the soma [4, 52]. These features unambiguously distinguish them from all other known types of RGCs in rabbits.

In vertical sections of the rabbit retina, immunofluorescence of the nAChR α4 and β2 subunits was observed as a distinctive pattern of labeling (Fig. 2). The nAChR α4 and β2 subunits are positioned mostly in the IPL and GCL. Some immunoreactivity of the nAChR α4 and β2 subunits was also dispersed in the outer plexiform layer (OPL) and the inner plexiform layer (INL). These results on the vertical distributions of the nAChR α4 and β2 subunits were similar to previous results [27, 28, 38]. Control tissues showed no the immunoreactivity of the nAChR α4 and β2 subunits (Fig. 2B, 2D). These results indicated that the anti-

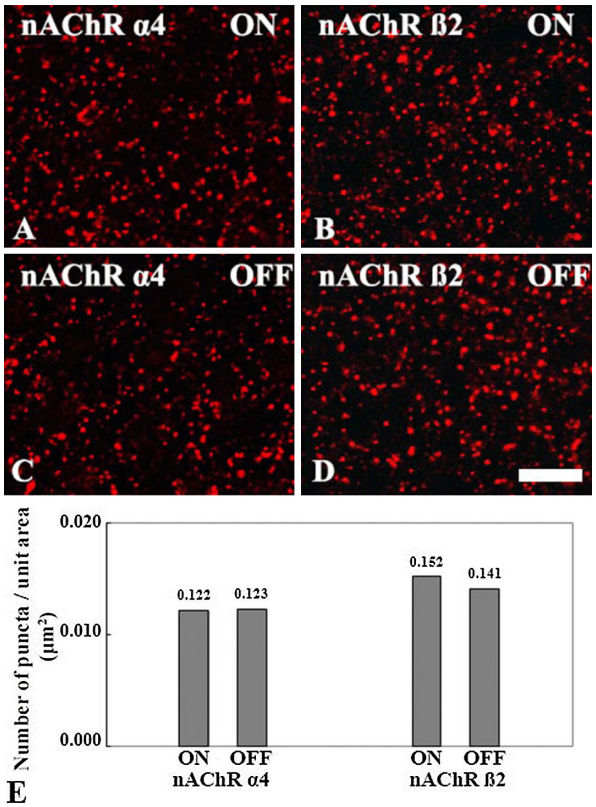

Fig. 3. Fluorescence confocal micrographs of the mid-peripheral rabbit retinal whole mounts that are immunolabeled with antibodies against the nAChR α4 and β2 subunits. The images in panels (**A**) and (**B**) were taken from the ON layer and the images in panels (**C**) and (**D**) were taken from the OFF layer. The graph (**E**) shows the calculated immunopuncta number per unit area. Bar = 10 μm.

bodies of the nAChR α4 and β2 subunits had the specificity for rabbit retina.

In whole mounts of rabbit retina (Fig. 3), immunoreactive puncta of the nAChR α4 and β2 subunits were located predominately in both of the ON and OFF sublamina of the IPL. All images in Figure 3 were taken from the mid-peripheral adult rabbit retina. We also calculated the number of immunopuncta, which were layered on the dendritic fields of the DS RGCs, to average the number of immunopuncta per unit area (Fig. 3E). The average number of nAChR α4 and β2 subunits immunopuncta was similar within both the ON and OFF layer (the nAChR α4 subunits in the ON layer was 0.122 and the nAChR α4 subunits in the OFF layer was 0.123; the nAChR β2 subunits in the ON layer was 0.152 and the nAChR β2 subunits in OFF layer was 0.141).

We used a double-labeling technique to identify the nAChR α4 and β2 subunits on the dendrites of the DS RGCs (Fig. 4). The nAChR β2 subunits (Green; Fig. 4A) and the dendrites of the Lucifer yellow-injected DS RGCs (Blue; Fig. 4B) are shown in the images. The two images are merged in Figure 4C, and the localization of the nAChR subunits immunopuncta upon the dendrites of DS RGC is shown in Figure 4D.

To reveal the distribution of the nAChR α4 and β2 subunits on the dendritic arbors of the ON and OFF DS RGCs, we reconstructed the entire distribution maps of the rabbit (Fig. 5). In each figure, the two panels in the left column show the distribution of the nAChR α4 (Fig. 5A) and β2 (Fig. 5D) subunits (Red dots) on the ON dendritic arbors (Black line). The middle column shows the distribution of the nAChR α4 (Fig. 5B) and β2 (Fig. 5E) subunits (Blue dots) on the OFF dendritic arbors (Green line). The panels of the right column are a merged images of the nAChR α4 (Fig. 5C) and β2 (Fig. 5F) subunits on both the ON and OFF dendritic arbors of the DS RGCs. The locations of the nAChR α4 and β2 on the dendritic arbors of the ON and OFF DS RGCs have no pattern. That is, they were distributed on the dendritic arbors in a seemingly random manner.

We calculated the number of nAChR α4 and β2 subunits immunoreactive puncta on the dendrites for each of the eight cardinal directions. Immunoreactive puncta within 45° of a given cardinal direction were included in Figure 6A. The histograms show the average densities of immunoreactive puncta/μm of dendrite that were calculated at 10 μm intervals from the center of the soma to the outer dendrites within each cardinal direction. The densities of the nAChR immunoreactive puncta were also expressed in terms of the average density of the immunoreactive puncta/total length (μm) of dendrites within each cardinal direction (Fig. 6C and 6D). In addition, we analyzed the average density of the nAChR immunoreactive puncta on whole dendrites for both the ON and OFF layers (Fig. 6B). The dendritic expression level of the nAChR α4 and β2 subunits was similar in both the ON and OFF layer (the nAChR α4

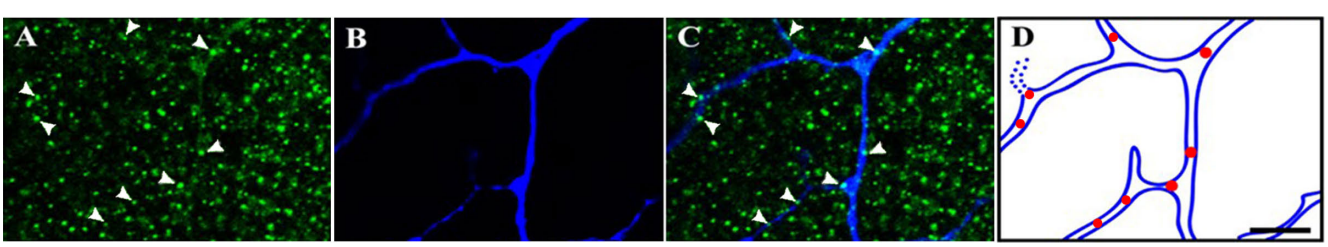

Fig. 4. Fluorescence confocal micrographs of the nAChR β2 subunits in the dendrites of the DS RGCs. The images in panels (**A**) and (**B**) show the immunolabeled nAChR β2 subunits and the dendrites of the DS RGCs, respectively. The arrowheads in (**C**) indicate the localization of the nAChR β2 subunits on the dendrites. The image in (**D**) shows the tracing of a dendrite and positioned nAChR immunopuncta. Bar = 10 μm.

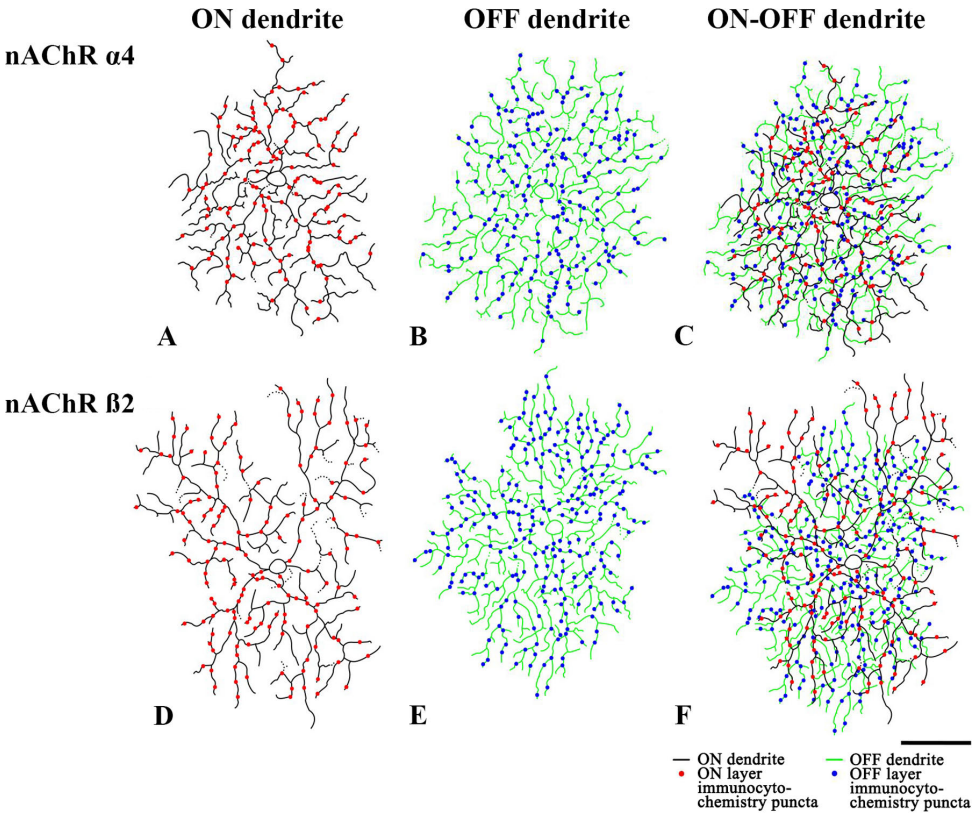

Fig. 5. Reconstructed images from digital photomicrographs show the distributions of the nAChR subunits on the ON (black line and red dots) and OFF (green line and blue dots) dendritic arbors of the DS RGCs. Bar = 100 μm.

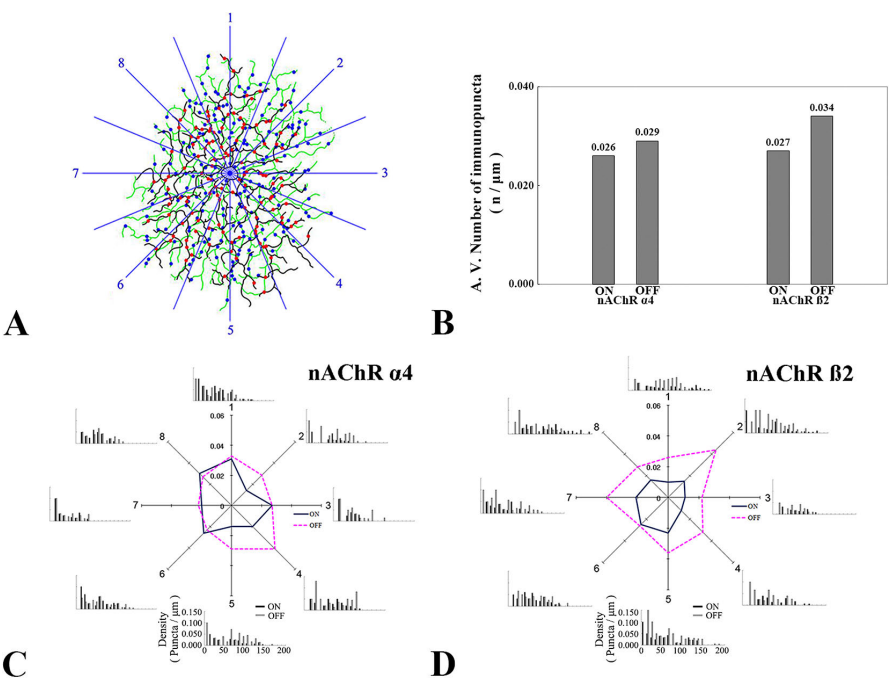

Fig. 6. The density histograms and average density graphs for each of the eight cardinal directions. (**A**) The method for separately calculating the distributions of the nAChR subunit immunoreactive puncta is shown for each of the eight cardinal directions. The graph in (**B**) shows the calculated immunopuncta number per unit distance. The central graphs (**C, D**) show the average density of immunoreactive puncta/total length of dendrites (μm) within each cardinal direction. The eight histograms surrounding the central graphs show the average density of the nAChR immunoreactive puncta at 10 μm intervals from the center of the soma to the outer dendrites within each cardinal direction.

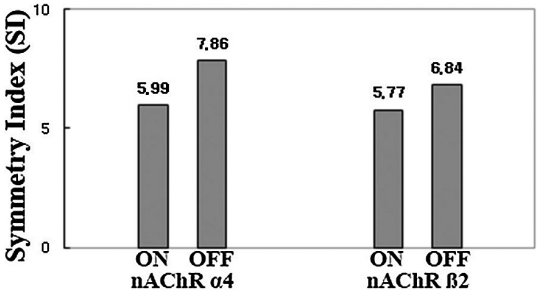

Fig. 7. A histogram showing the symmetry index (SI) for the spatial density of the nAChR immunoreactive puncta on the ON and OFF dendritic arbors of the direction-selective retinal ganglion cells. The SI value of 10 indicates complete symmetry, and the SI value of 0 indicates no symmetry.

subunits in the ON layer was 0.026 and the nAChR α4 subunits in the OFF layer was 0.029; the nAChR β2 subunits in the ON layer was 0.027 and the nAChR β2 subunits in OFF layer was 0.034). The distribution of the localized immunopuncta of the nAChR subunits showed as typically nonuniform pattern, with no evidence of an asymmetrical pattern.

The SI estimates the precise spatial symmetry of a given component [41]. We calculated the SI for each cell to measure how evenly the spatial density of nAChR immunoreactive puncta was distributed throughout the dendritic arbors of the DS RGCs (n = 2 cells, N = 1 animal). Figure 7 shows the SI for the spatial density of the nAChR immunoreactive puncta on the ON and OFF dendritic arbors of DS RGCs. The SI of the nAChR α4-immunoreactive puncta was 5.99 (ON dendritic arbors) and 7.86 (OFF dendritic arbors). The SI of the nAChR β2-immunoreactive puncta was 5.77 (ON dendritic arbors) and 6.84 (OFF dendritic arbors). These results demonstrate that the distributions of the nAChR α4 and β2 subunits are not asymmetric in both the ON and OFF dendrites of the DS RGCs.

IV. Discussion

In the present study, we analyzed the distributional pattern of the nAChR α4 and β2 subunits on the dendrites of the ON-OFF DS RGCs in the adult rabbit retina. The expression of the nAChR subunits has been investigated in the retina and visual cortex through electrophysiological techniques and immunocytochemistry [27, 35, 51]. These nAChR subunits play critical roles in the visual system. Deletion of the gene for the nAChR α7 subunit in knockout mice impairs visual cortical function and visual acuity [40]. In addition, many anatomical and pharmacological investigations have revealed that the various subunits of the nAChR contribute to direction selectivity in the mammalian retina [7, 29, 45, 50]. The nAChRs are located on dendrites of the DS RGCs, and mediate 30–50% of the excitatory inputs of the DS RGCs [7, 29, 36]. Additionally, a nAChRs antagonist, curare, reduces direction selectivity [7, 21, 29, 50]. These previous studies suggest that identifying the distributional pattern of the nAChR subunits on the dendrites of the DS RGCs may be useful for providing evidence of the mechanism underlying the direction-selective retinal circuit.

Analysis of the distributional pattern of specific receptors contributes to the establishment of the major mechanism for direction selectivity by demonstrating the structural and physiological properties of the DS RGCs [10, 34, 49]. In particular, through research on the asymmetric distributional pattern of functional GABAergic input from the SACs onto the dendrites of DS RGCs, which demonstrated the influence of the SACs on null direction inhibition, a prominent theory called the ‘push-pull’ model has been formulated and developed. The theory suggests that direction selectivity is pushed by the excitatory inputs of the bipolar cells and SACs, and partially pulled by the inhibitory input of the SACs onto the DS RGCs [10, 34, 47]. In a recent study, there was a meaningful result with the anatomical pattern of specific nAChR subunits that the expressional pattern of the nAChR α7 and β2 subunits on the dendritic arbors of the ON-OFF DS RGCs in the mouse retina were anisotropic at postnatal day 5, but not after postnatal day 10 [28]. These results show how direction-selective circuits involving the SACs and DS RGCs are formed during early postnatal development, and how their anatomical connectivity changes through retinal maturation. We also focused on analysis with a distributional pattern of the specific nAChR subunits. Our present results may indicate that the nAChR α4 and β2 subunits do not directly influence on the induction of direction selectivity because of the non-asymmetrical expressing pattern of nAChR α4 and β2 subunits upon dendrites of ON-OFF DS RGCs in adult rabbit retina.

We previously reported that most glutamate receptors, including N-methyl-D-aspartate (NMDA), α-amino-3-hydroxy-5-methyl-4-isoxazole propionate (AMPA), and kainate (KA) receptors, showed no anatomical evidence of asymmetry in their distribution patterns on the dendrites of the ON-OFF DS RGCs in the adult rabbit retina [26, 30, 31]. Taken together, our previous and present expressional pattern results indicate that the excitatory neurotransmitters receptor subunits have no critical effect on the anisotropy of the ON-OFF DS RGCs for the induction of direction selectivity. Therefore, additional studies may be required that investigate the integrative cellular connectivity between the DS RGCs and their surrounding cells. The DS RGCs receive excitatory cholinergic and glutamatergic neurotransmitters from the SACs and bipolar cells in the mammalian retina, respectively [13, 17, 37, 49]. Although various excitatory neurotransmitters are secreted from different cells onto the DS RGCs, the distributional patterns of excitatory neurotransmitters receptor subunits upon the dendritic arbors of the ON-OFF DS RGCs in the adult rabbit retina are not asymmetric. This finding suggests that there is a specific mechanism for maintaining a balance in

excitatory input among the surrounding cells of the DS RGCs. Several studies have focused on identifying how a balance of excitation and inhibition is maintained in this direction-selective circuit [14, 20, 23, 43]. Thus, future studies may ultimately propose multiple complex mechanisms for the induction of direction selectivity.

The vertical distribution of the nAChR α4 and β2 subunits was different. The expression of the nAChR α4 subunit was more intense at the GCL than the IPL (Fig. 2A), and nAChR β2 subunits showed a bias toward expression in the IPL (Fig. 2C). A similar expressional pattern was found for the immunoreactive puncta of the nAChR α4 and β2 subunits in the ON and OFF layers (Fig. 3E). In general, these two nAChR subunits usually form a heteromeric nAChR receptor [1, 35, 48]; however, these two subunits were expressed at different levels in the GCL. Therefore, we speculated that these two distinct types of the nAChR subunits have different roles in the GCL of the adult rabbit retina. One possible rationale for their expressional difference is that the α4 subunit might combine with other subunits (i.e. β3 or β4). Different assemblies of the nAChR subunits have different pharmacological profiles; for example, an α and non-α subunit composition contribute to the binding site [1]. Diverse compositions of the nAChR subunits characterize not only neuronal subtypes but also the anatomical compartment of a single neuron [1]. Inhibitory synapses typically occur at the peri-somatic position for efficient repression of post-neuronal activity. Indeed, the α4 subunit of the nAChR can directly modulate inhibitory postsynaptic potentials (IPSCs) of GABAergic synapses on pyramidal neurons in cortex layer V [6]. However, we still do not know the subunit types that are co-expressed with the α4 subunit in the GCL of the adult rabbit retina. Cox and his colleagues revealed the diversity of the nAChRs in the rat optic nerve, which initiates from the retinal ganglion cells. Moreover, the α4 subunit of the nAChR are able to compose with the α6 and β3 subunits [12]. For this reason, future studies are needed to identify the binding partner of the α4 subunit of the nAChR, and to determine whether it is located at the inhibitory synapses of the adult rabbit retina.

In conclusion, we revealed the overall expressional patterns of the nAChR α4 and β2 subunits upon both the ON and OFF dendrites of the DS RGCs in the adult rabbit retina. The distributional pattern of the nAChR α4 and β2 subunits was not asymmetric, which implies that these subunits have an indirect influence on the formation of direction selectivity in the retina. Our present results provide fundamental information of the anatomical distributions of the excitatory nAChRs components in the ON and OFF dendrites of the DS RGCs within the adult rabbit retina, which may be useful to describe the mechanism of direction selectivity.

V. Acknowledgments

We thank Cactus Communications for proofreading the manuscript. This research was supported by Kyungpook National University Bokhyeon Research Fund, 2015.

VI. References

1. Albuquerque, E. X., Pereira, E. F., Alkondon, M. and Rogers, S. W. (2009) Mammalian nicotinic acetylcholine receptors: from structure to function. *Physiol. Rev.* 89; 73–120.
2. Ames, A. and Nesbett, F. B. (1981) In vitro retina as an experimental model of the central nervous system. *J. Neurochem.* 37; 867–877.
3. Amthor, F. R., Oyster, C. W. and Takahashi, E. S. (1984) Morphology of on-off direction-selective ganglion cells in the rabbit retina. *Brain Res.* 298; 187–190.
4. Amthor, F. R., Takahashi, E. S. and Oyster, C. W. (1989) Morphologies of rabbit retinal ganglion cells with complex receptive fields. *J. Comp. Neurol.* 280; 97–121.
5. Amthor, F. R., Keyser, K. T. and Dmitrieva, N. A. (2002) Effects of the destruction of starburst-cholinergic amacrine cells by the toxin AF64A on rabbit retinal directional selectivity. *Vis. Neurosci.* 19; 495–509.
6. Aracri, P., Consonni, S., Morini, R., Perrella, M., Rodighiero, S., Amadeo, A. and Becchetti, A. (2010) Tonic modulation of GABA release by nicotinic acetylcholine receptors in layer V of the murine prefrontal cortex. *Cereb. Cortex* 20; 1539–1555.
7. Ariel, M. and Daw, N. W. (1982) Effects of cholinergic drugs on receptive field properties of rabbit retinal ganglion cells. *J. Physiol.* 324; 135–160.
8. Barlow, H. B. and Hill, R. M. (1963) Selective sensitivity to direction of movement in ganglion cells of the rabbit retina. *Science* 139; 412–414.
9. Barlow, H. B., Hill, R. M. and Levick, W. R. (1964) Retinal ganglion cells responding selectively to direction and speed of image motion in the rabbit. *J. Physiol.* 173; 377–407.
10. Briggman, K. L., Helmstaedter, M. and Denk, W. (2011) Wiring specificity in the direction-selectivity circuit of the retina. *Nature* 471; 183–188.
11. Chan, Y. C. and Chiao, C. C. (2013) The distribution of the preferred directions of the on-off direction selective ganglion cells in the rabbit retina requires refinement after eye opening. *Physiol. Rep.* 1; e00013.
12. Cox, B. C., Marritt, A. M., Perry, D. C. and Kellar, K. J. (2008) Transport of multiple nicotinic acetylcholine receptors in the rat optic nerve: high densities of receptors containing α6 and β3 subunits. *J. Neurochem.* 105; 1924–1938.
13. Demb, J. B. (2007) Cellular mechanisms for direction selectivity in the retina. *Neuron* 55; 179–186.
14. Enciso, G. A., Rempe, M., Dmitriev, A. V., Gavrikov, K. E., Terman, D. and Mangel, S. C. (2010) A model of direction selectivity in the starburst amacrine cell network. *J. Comput. Neurosci.* 28; 567–578.
15. Euler, T., Detwiler, P. B. and Denk, W. (2002) Directionally selective calcium signals in dendrites of starburst amacrine cells. *Nature* 418; 845–852.
16. Famiglietti, E. V. (1991) Synaptic organization of starburst amacrine cells in rabbit retina: analysis of serial thin sections by electron microscopy and graphic reconstruction. *J. Comp. Neurol.* 309; 40–70.
17. Famiglietti, E. V. and Tumosa, N. (1987) Immunocytochemical staining of cholinergic amacrine cells in rabbit retina. *Brain Res.* 413; 398–403.
18. Fried, S. I., Münch, T. A. and Werblin, F. S. (2002) Mechanisms and circuitry underlying directional selectivity in the retina. *Nature* 420; 411–414.
19. Grzywacz, N. M., Amthor, F. R. and Merwine, D. K. (1998) Necessity of acetylcholine for retinal directionally selective

responses to drifting gratings in rabbit. *J. Physiol.* 512; 575–581.
20. Hausselt, S. E., Euler, T., Detwiler, P. B. and Denk, W. (2007) A dendrite-autonomous mechanism for direction selectivity in retinal starburst amacrine cells. *PLoS Biol.* 5; e185.
21. He, S. and Masland, R. H. (1997) Retinal direction selectivity after targeted laser ablation of starburst amacrine cells. *Nature* 389; 378–382.
22. He, S., Dong, W., Deng, Q., Weng, S. and Sun, W. (2003) Seeing more clearly: recent advances in understanding retinal circuitry. *Science* 302; 408–411.
23. Hoggarth, A., McLaughlin, A. J., Ronellenfitch, K., Trenholm, S., Vasandani, R., Sethuramanujam, S., Schwab, D., Briggman, K. L. and Awatramani, G. B. (2015) Specific wiring of distinct amacrine cells in the directionally selective retinal circuit permits independent coding of direction and size. *Neuron* 86; 276–291.
24. Jeon, C. J., Strettoi, E. and Masland, R. H. (1998) The major cell populations of the mouse retina. *J. Neurosci.* 18; 8936–8946.
25. Jeon, C. J., Kong, J. H., Strettoi, E., Rockhill, R., Stasheff, S. F. and Masland, R. H. (2002) Pattern of synaptic excitation and inhibition upon direction-selective retinal ganglion cells. *J. Comp. Neurol.* 449; 195–205.
26. Jeong, S. A., Kwon, O. J., Lee, J. Y., Kim, T. J. and Jeon, C. J. (2006) Synaptic pattern of AMPA receptor subtypes upon direction-selective retinal ganglion cells. *Neurosci. Res.* 56; 427–434.
27. Keyser, K. T., MacNeil, M. A., Dmitrieva, N., Wang, F., Masland, R. H. and Lindstrom, J. M. (2000) Amacrine, ganglion, and displaced amacrine cells in the rabbit retina express nicotinic acetylcholine receptors. *Vis. Neurosci.* 17; 743–752.
28. Kim, H. J. and Jeon, C. J. (2014) Synaptic pattern of nicotinic acetylcholine receptor α7 and β2 subunits on the direction-selective retinal ganglion cells in the postnatal mouse retina. *Exp. Eye Res.* 122; 54–64.
29. Kittila, C. A. and Massey, S. C. (1997) Pharmacology of directionally selective ganglion cells in the rabbit retina. *J. Neurophysiol.* 77; 675–689.
30. Kwon, O. J., Kim, M. S., Kim, T. J. and Jeon, C. J. (2007) Identification of synaptic pattern of kainate glutamate receptor subtypes on direction-selective retinal ganglion cells. *Neurosci. Res.* 58; 255–264.
31. Kwon, O, J., Lee, J. S., Kim, H. G. and Jeon, C. J. (2016) Identification of synaptic patterns of NMDA receptor subtypes upon direction-selective rabbit retinal ganglion cells. *Curr. Eye Res.* 41; 832–843.
32. Lee, J. G., Lee, K. P. and Jeon, C. J. (2012) Synaptic pattern of KA1 and KA2 upon the direction-selective ganglion cells in developing and adult mouse retina. *Acta Histochem. Cytochem.* 45; 35–45.
33. Lee, S. and Zhou, Z. J. (2006) The synaptic mechanism of direction selectivity in distal processes of starburst amacrine cells. *Neuron* 51; 787–799.
34. Lee, S., Kim, K. and Zhou, Z. J. (2010) Role of ACh-GABA cotransmission in detecting image motion and motion direction. *Neuron* 68; 1159–1172.
35. Lindstrom, J. (1996) Neuronal nicotinic acetylcholine receptors. *Ion Channels* 4; 377–450.
36. Masland, R. H. and Ames, A. (1976) Responses to acetylcholine of ganglion cells in an isolated mammalian retina. *J. Neurophysiol.* 39; 1220–1235.
37. Masland, R. H., Mills, J. W. and Hayden, S. A. (1984) Acetylcholine-synthesizing amacrine cells: identification and selective staining by using radioautography and fluorescent markers. *Proc. R. Soc. Lond. B Biol. Sci.* 223; 79–100.
38. Moretti, M., Vailati, S., Zoli, M., Lippi, G., Riganti, L., Longhi, R., Viegi, A., Clementi, F. and Gotti, C. (2004) Nicotinic acetylcholine receptor subtypes expression during rat retina development and their regulation by visual experience. *Mol. Pharmacol.* 66; 85–96.
39. O'Malley, D. M., Sandell, J. H. and Masland, R. H. (1992) Co-release of acetylcholine and GABA by the starburst amacrine cells. *J. Neurosci.* 12; 1394–1408.
40. Origlia, N., Valenzano, D. R., Moretti, M., Gotti, C. and Domenici, L. (2012) Visual acuity is reduced in alpha 7 nicotinic receptor knockout mice. *Invest. Ophthalmol. Vis. Sci.* 53; 1211–1218.
41. Panno, J. P. (1988) Symmetry analysis of cell nuclei. *Cytometry* 9; 195–200.
42. Pei, Z., Chen, Q., Koren, D., Giammarinaro, B., Acaron Ledesma, H. and Wei, W. (2015) Conditional knock-out of vesicular GABA transporter gene from starburst amacrine cells reveals the contributions of multiple synaptic mechanisms underlying direction selectivity in the retina. *J. Neurosci.* 35; 13219–13232.
43. Poleg-Polsky, A. and Diamond, J. S. (2016) Retinal circuitry balances contrast tuning of excitation and inhibition to enable reliable computation of direction selectivity. *J. Neurosci.* 36; 5861–5876.
44. Sigal, Y. M., Speer, C. M., Babcock, H. P. and Zhuang, X. (2015) Mapping synaptic input fields of neurons with super-resolution imaging. *Cell* 163; 493–505.
45. Strang, C. E., Renna, J. M., Amthor, F. R. and Keyser, K. T. (2007) Nicotinic acetylcholine receptor expression by directionally selective ganglion cells. *Vis. Neurosci.* 24; 523–533.
46. Sun, W., Li, N. and He, S. (2002) Large-scale morphological survey of mouse retinal ganglion cells. *J. Comp. Neurol.* 451; 115–126.
47. Vaney, D. I. and Taylor, W. R. (2002) Direction selectivity in the retina. *Curr. Opin. Neurobiol.* 12; 405–410.
48. Wang, F., Gerzanich, V., Wells, G. B., Anand, R., Peng, X., Keyser, K. and Lindstrom, J. (1996) Assembly of human neuronal nicotinic receptor α5 subunits with α3, β2, and β4 subunits. *J. Biol. Chem.* 271; 17656–17665.
49. Wei, W. and Feller, M. B. (2011) Organization and development of direction-selective circuits in the retina. *Trends Neurosci.* 34; 638–645.
50. Weng, S., Sun, W. and He, S. (2005) Identification of on-off direction-selective ganglion cells in the mouse retina. *J. Physiol.* 562; 915–923.
51. Whiting, P. J., Schoepfer, R., Conroy, W. G., Gore, M. J., Keyser, K. T., Shimasaki, S., Esch, F. and Lindstrom, J. M. (1991) Expression of nicotinic acetylcholine receptor subtypes in brain and retina. *Brain Res. Mol. Brain Res.* 10; 61–70.
52. Yang, G. and Masland, R. H. (1992) Direct visualization of the dendritic and receptive fields of directionally selective retinal ganglion cells. *Science* 258; 1949–1952.
53. Yang, G. and Masland, R. H. (1994) Receptive fields and dendritic structure of directionally selective retinal ganglion cells. *J. Neurosci.* 14; 5267–5280.
54. Yi, C. W., Yu, S. H., Lee, E. S., Lee, J. G. and Jeon, C. J. (2012) Types of parvalbumin-containing retinotectal ganglion cells in mouse. *Acta Histochem. Cytochem.* 45; 201–210.
55. Yonehara, K., Balint, K., Noda, M., Nagel, G., Bamberg, E. and Roska, B. (2011) Spatially asymmetric reorganization of inhibition establishes a motion-sensitive circuit. *Nature* 469; 407–410.
56. Yoshida, K., Watanabe, D., Ishikane, H., Tachibana, M., Pastan, I. and Nakanishi, S. (2001) A key role of starburst amacrine cells in originating retinal directional selectivity and optokinetic eye movement. *Neuron* 30; 771–780.
57. Zhou, Z. J. and Lee, S. (2008) Synaptic physiology of direction selectivity in the retina. *J. Physiol.* 586; 4371–4376.